PASJ: Publ. Astron. Soc. Japan , 1–??,

Astrometry of Galactic Star-Forming Region Onsala 1 with VERA: Estimation of Angular Velocity of Galactic Rotation at Sun

Takumi Nagayama,[1] Toshihiro Omodaka,[2] Akiharu Nakagawa,[2] Toshihiro Handa,[3]
Mareki Honma,[1] Hideyuki Kobayashi,[1] Noriyuki Kawaguchi,[1] and Takeshi Miyaji[1]
[1]*Mizusawa VLBI Observatory, National Astronomical Observatory of Japan, 2-21-1 Osawa, Mitaka, Tokyo 181-8588*
takumi.nagayama@nao.ac.jp
[2]*Graduate School of Science and Engineering, Kagoshima University, 1-21-35 Kôrimoto, Kagoshima, Kagoshima 890-0065*
[3]*Institute of Astronomy, The Universe of Tokyo, 2-21-1 Osawa, Mitaka, Tokyo 181-0015*

(Received 2010 June 18; accepted 2010 December 1)

Abstract

We conducted the astrometry of H_2O masers in the Galactic star-forming region Onsala 1 (ON1) with VLBI Exploration of Radio Astrometry (VERA). We measured a trigonometric parallax of 0.404 ± 0.017 mas, corresponding to a distance of 2.47 ± 0.11 kpc. ON1 is appeared to be located near the tangent point at the Galactic longitude of 69.°54. We estimate the angular velocity of the Galactic rotation at Sun, the ratio of the distance from Sun to the Galactic center and the Galactic rotation velocity at Sun, to be $\Omega_0 = \Theta_0/R_0 = 28.7 \pm 1.3$ km s^{-1} kpc^{-1} using the measured distance and proper motion of ON1. This value is larger than the IAU recommended value of 220 km s^{-1}/8.5 kpc = 25.9 km s^{-1} kpc^{-1}, but consistent with other results recently obtained with the VLBI technique.

Key words: Astrometry:— ISM: individual (Onsala1) — masers (H_2O)

1. Introduction

Very Long Baseline Interferometry (VLBI) astrometry is an important method to measure the structure of the Milky Way Galaxy (MWG). By measuring the accurate position of the source and its time variation, the source distance and proper motion could be determined directly. VLBI astrometry at 10 μas accuracy of the Galactic H_2O and CH_3OH maser sources with VLBI Exploration of Radio Astrometry (VERA) and Very Long Baseline Array (VLBA) determined accurate distances at kpc-scale with the errors less than 10% (see for example Hachisuka et al. 2006; Xu et al. 2006; Honma et al. 2007).

The Galactic constants, the distance from Sun to the Galactic center (R_0) and the Galactic rotation velocity at Sun (Θ_0) are major parameters to study the structure of the MWG. The rotation curve of the MWG and all kinematic distances of the sources in the MWG are based directly on the Galactic constants. Although International Astronomical Union (IAU) has recommended to give the values of $R_0 = 8.5$ kpc and $\Theta_0 = 220$ km s^{-1} since 1985, numerous recent studies report the values different from them (e.g. Reid et al. 2009).

However, observational estimation of the Galactic constants is difficult. This is because the observational estimation of Galactic constants is affected by several independent assumptions; the peculiar motion of the source, systemic non-circular motions of both the source and the LSR due to the spiral arm and the non-axisymmetric potential of the MWG, and relative motion of Sun to the LSR (Reid et al. 2009; McMillan & Binney 2010). To minimize these effects, we should observe many sources located at various positions in the MWG.

The tangent point that the vector of the source Galactic rotation is parallel to the line of sight is a kinematically unique position in the MWG. In the case that the source is located at this point and on the pure circular rotation, the proper motion of the source depends only on the Galactic rotation of Sun, Θ_0. Therefore, we can estimate Θ_0 from the measured proper motion. We can also estimate R_0 from the measured source distance, since the tangent point, Sun, and the Galactic center make the right triangle. Sato et al. (2010) measured the parallactic distance of W51 Main/South which is located near the tangent point, and estimated $R_0 = 8.3 \pm 1.1$ kpc using this simple geometry. Even if the source is not located at the tangent point, but near there, we can estimate the ratio of Galactic constants, Θ_0/R_0, the angular velocity of the Galactic rotation at Sun, Ω_0, as described in Section 4. The value of this ratio is a constraint to estimate one of the Galactic constants from the other. Although the IAU gives recommended values of the Galactic constants, at least one of them should be revised, if the ratio is inconsistent to the observed value.

The radial velocity of the source located at the tangent point is equal to the terminal velocity. It is defined as the extreme velocity on any line of sight at $b \simeq 0°$, and described as $v_{\rm term} = \Theta - \Theta_0 \sin l$, where Θ is the Galactic rotation velocity of the source. Therefore, we selected the sources whose radial velocities are close to the terminal velocity. One of these sources, Onsala 1 (ON1) is a massive star-forming region located at the Galactic coor-

dinate of $(l, b) = (69.^\circ54, -0.^\circ98)$. The radial velocity of ON1 is close to the terminal velocity. The radial velocity observed in molecular lines is 12 ± 1 km s^{-1} (Bronfman et al. 1996; Pankonin et al. 2001). The terminal velocity at $l = 69.^\circ54$ is derived to be 14 km s^{-1} from the IAU recommended value of $\Theta_0 = 220$ km s^{-1} and assuming the flat rotation ($\Theta = \Theta_0$), and is 15 ± 5 km s^{-1} in the l-v diagram of Dame et al. (2001). The distance of ON1 is measured to be $2.57^{+0.34}_{-0.27}$ kpc by the 6.7 GHz CH_3OH maser astrometry with the EVN (Rygl et al. 2010). VLBI maps of the H_2O masers have been reported by Nagayama et al. (2008). They found that ON1 has two clusters of H_2O masers (WMC1 and WMC2) separated by $1.''6$.

In the present study, we report on our successful determination of the parallax of ON1 with VERA. This is a first step to estimate the Galactic constants and the angular velocity of the Galactic rotation at Sun using VERA.

2. Observations and Reductions

We observed H_2O masers in the star-forming region ON1 with VERA at 11 epochs spanned about two years. The epochs are day of year (DOY) 245, 256, 290, 309, 360 in 2006, 046, 091, 129, 223 in 2007, 020, and 202 in 2008. At each epoch, the H_2O 6_{16}-5_{23} maser at a rest frequency of 22.235080 GHz in ON1 and a position reference source J2010+3322 were simultaneously observed in a dual-beam mode for about 10 hours. The typical on-source integration time was 6 hours for both ON1 and J2010+3322. J2010+3322 is listed in VLBA Calibrator Survey 2 (VCS2: Fomalont et al. 2003). J2010+3322 was detected with a peak flux density of 100–130 mJy in each epochs. The separation angle between ON1 and J2010+3322 is $1.^\circ85$. The instrumental phase difference between the two beams was measured continuously during the observations by injecting artificial noise sources into both beams (Honma et al. 2008). Left-hand circular polarization signals were sampled with 2-bit quantization, and filtered with the VERA digital filter unit (Iguchi et al. 2005). The data were recorded onto magnetic tapes at a rate of 1024 Mbps, providing a total bandwidth of 256 MHz, which consists of 16×16 MHz IF channels. One IF channel was assigned to ON1, and the other 15 IF channels were assigned to J2010+3322, respectively. Correlation processing was carried out on the Mitaka FX correlator. The frequency and velocity resolutions for ON1 were 31.25 kHz and 0.42 km s^{-1}, respectively.

Data reduction was conducted using the NRAO Astronomical Image Processing System (AIPS). An amplitude calibration was performed using the system noise temperatures during the observations. For phase-referencing, a fringe fitting was made using the AIPS task FRING on J2010+3322 with a typical integration time of 2 min. The solutions of the fringe phases, group delays, and delay rates were obtained every 30 sec. These solutions were applied to the data of ON1 in order to calibrate the visibility data. Phase and amplitude solutions obtained from self-calibration of J2010+3322 were also applied to ON1. Visibility phase errors caused by the Earth's atmosphere were calibrated based on GPS measurements of the atmospheric zenith delay which occurs due to tropospheric water vapor (Honma et al. 2008). After the calibration, we made spectral-line image cubes using the AIPS task IMAGR around masers with 1024×1024 pixels of size 0.05 milliarcsecond (mas). The typical size of the synthesized beam was 1.3×0.9 mas with position angle of -40°. The rms noises for each images were approximately 0.1–1 Jy beam^{-1}. The signal-to-noise ratio of 7 was adopted as the detection criterion.

In the single-beam VLBI imaging of ON1 (without phase-referencing to the J2010+3322 in the other beam), group delays solved on J2025+3343 in the same beam were applied. The fringe fitting was done using one of the brightest emissions at LSR velocity of 14.9 km s^{-1} in ON1, and the solutions are applied to all velocity channels. The data reductions for single-beam imaging are the same method with previous JVN observations of ON1 (Nagayama et al. 2008).

3. Results

3.1. Overall Properties of H_2O Masers in ON1

Figure 1 shows the scalar-averaged cross-power spectra of ON1 H_2O masers in approximately half a year intervals. They are obtained with the Mizusawa-Iriki baseline, and averaged for the total observational time. There are low-velocity components ($v_{\rm LSR} = -7$ to 17 km s^{-1}) near the systemic velocity of ON1 ($v_{\rm LSR} = 12 \pm 1$ km s^{-1}; Bronfman et al. 1996), and high-velocity blue-shifted ($v_{\rm LSR} = -57$ to -32 km s^{-1}) and red-shifted ($v_{\rm LSR} = 55$ to 70 km s^{-1}) components. The most of the low-velocity components are detected over one year. The high-velocity components are time-variable and not persistent for more than half a year.

We detected 28 H_2O maser features for more than two epochs. Figure 2 shows the distributions and internal motions of these features. The masers are distributed with approximately $1'' \times 2''$ area, which is consistent with the previous VLBI observations (Nagayama et al. 2008). The difference between the present and previous observations is the difference in time intervals of the epochs. By observing with the shorter time intervals of 1–2 months, the number of the maser features which we can trace the internal motions in the present observations increased to the twice of the previous ones. ON1 has two clusters of H_2O maser features located at $(x, y) \simeq (0.''0, 0.''0)$ and $(-0.''9, -1.''4)$. They are named as WMC1 and WMC2 by Nagayama et al. (2008), respectively.

The internal motions of WMC1 exhibit a bipolar outflow structure in the east-west direction. The blue- and red-shifted features show the high expansion velocity of $\simeq$ 70 km s^{-1} in three-dimensional velocity. The low velocity features with $v_{\rm LSR} = -7$ to 17 km s^{-1} show low expansion velocity of $\simeq$ 10 km s^{-1}. In the previous observations, the blue- and red-shifted features were distributed within two small regions of approximately 15×15 mas separated by $\simeq$ 200 mas, and were not detected outside of these regions (Nagayama et al. 2008). They are two clusters of

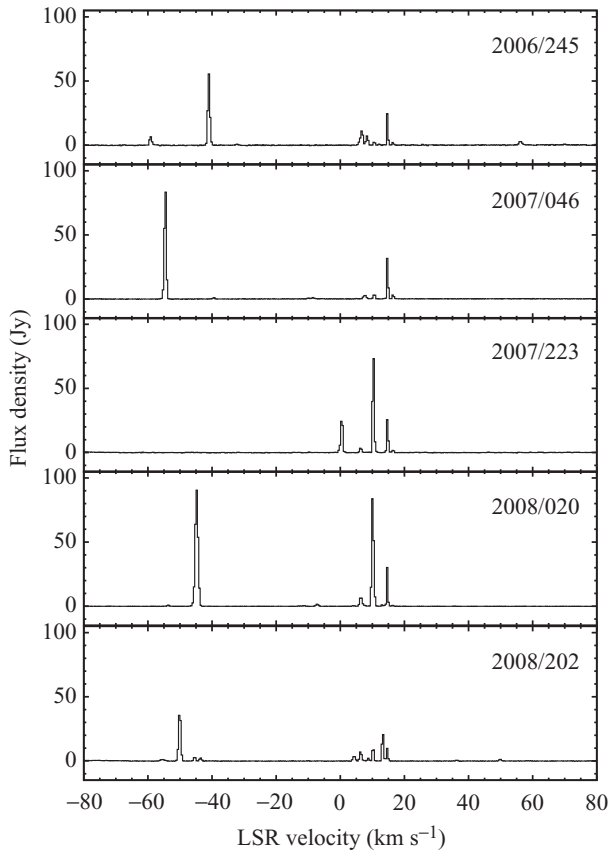

Fig. 1. Scalar-averaged cross-power spectra of the ON1 H_2O masers obtained with Mizusawa-Iriki baseline.

the blue-shifted features around $(x, y) \simeq (-5, 45)$ mas and the red-shifted features around $(-200, 50)$ mas in Figure 2(b). Nagayama et al. (2008) suggest that a driving source of H_2O masers is located near the midpoint of these two clusters. However, we detected a new red-shifted feature at $(x, y) \simeq (-40, 45)$ mas. Therefore, the driving source would be located between the cluster of blue-shifted features and a new red-shifted feature. In WMC2, only the low velocity features ($v_{\rm LSR} = 6$ to 14 km s^{-1}) are detected. Their internal motions did not show a systematic, and thus masers in WMC2 are not likely to originate from WMC1. We confirmed that there are two driving sources of H_2O masers in ON1.

3.2. Parallax and Proper Motion

Absolute motions of H_2O masers to the extragalactic position reference source are expressed by the sum of a linear motion and the trigonometric parallax. We conducted monitoring observations of H_2O masers for about two years, and their absolute motions were successfully obtained by referencing to the position reference source, J2010+3322. Figure 3 shows positional variations of one of the brightest maser feature at $v_{\rm LSR} = 14.9$ km s^{-1}. The positional variations show systematic sinusoidal modulation with a period of one year caused by the parallax.

In order to obtain the parallax and proper motion, we use the positions of ten maser features detected over half a year. We conducted a combined parallax fit, in which the positions of ten features are fitted simultaneously with one common parallax but different proper motions and position offsets for each spot. For this fit, we used errors of 0.057 and 0.082 mas in right ascension and declination, respectively, in quadrature to the formal fitting errors. This resulted in χ^2 per degree of freedom values of unity for both the right ascension and declination data. The resulting parallax is 0.404 ± 0.012 mas. Table 1 shows the results of the combined parallax fit.

To confirm the consistency of the parallax motion for each maser feature, we also estimate the parallax individually. In Table 1, we also show the obtained parallaxes using individual fitting for each maser feature. The obtained parallaxes of ten maser features are consistent with each other, from 0.382 to 0.428 mas, and give the similar result of 0.404 ± 0.012 mas.

Combining the results of ten maser features can lead to underestimation of the parallax uncertainty, in the case that the measurements are correlated among different maser features. Random-like errors such as map noise and maser feature structure variation would not be correlated among different maser features. However, systemic errors (e.g. from the correlator model or the atmosphere) would affect all maser features in one epoch in a very similar way. The conservative approach would be that the uncertainty is not reduced when the combined fitting of ten maser features are made. In this approach, the uncertainty would be estimated to be 0.021 mas from the smallest uncertainty of ID 3 maser feature. However, the results of ten maser features are not entirely correlated, since the obtained parallaxes from individual fitting are not completely the same value. Therefore, we estimate the final uncertainty of the parallax by taking the middle between the uncertainties of 0.012 and 0.021 mas, and obtain 0.404 ± 0.017 mas, which we adopt for the parallax of ON1.

The obtained parallax corresponds to a source distance of 2.47 ± 0.11 kpc. This distance is consistent with the 6.7 GHz CH_3OH maser parallax corresponding to $2.57^{+0.34}_{-0.27}$ kpc measured by Rygl et al. (2010), but it is obtained with 2 times higher accuracy. Figure 4 shows the position of ON1 in the MWG which is determined from the distance of 2.47 ± 0.11 kpc, the longitude of $l = 69.^{\circ}54$ and $R_0 = 8.5$ kpc. ON1 is appeared to be located on the Local arm and near the tangent point at $l = 69.^{\circ}54$.

The absolute proper motion of a maser feature is the sum of the internal motion of the maser feature, the Galactic rotation, the Solar motion, and the peculiar motion of the source. All motions expect the internal motion are common to all maser features. Therefore, the average of the absolute proper motions of maser features should give the systemic proper motion of the whole source, if the internal motions are randomized well. We consider that it is valid for ON1 because the averaged radial velocity of ten maser features is 11.1 km s^{-1}, and it is consistent with the systemic radial velocity derived from the associated molecular cloud ($v_{\rm LSR} = 12 \pm 1$ km s^{-1};

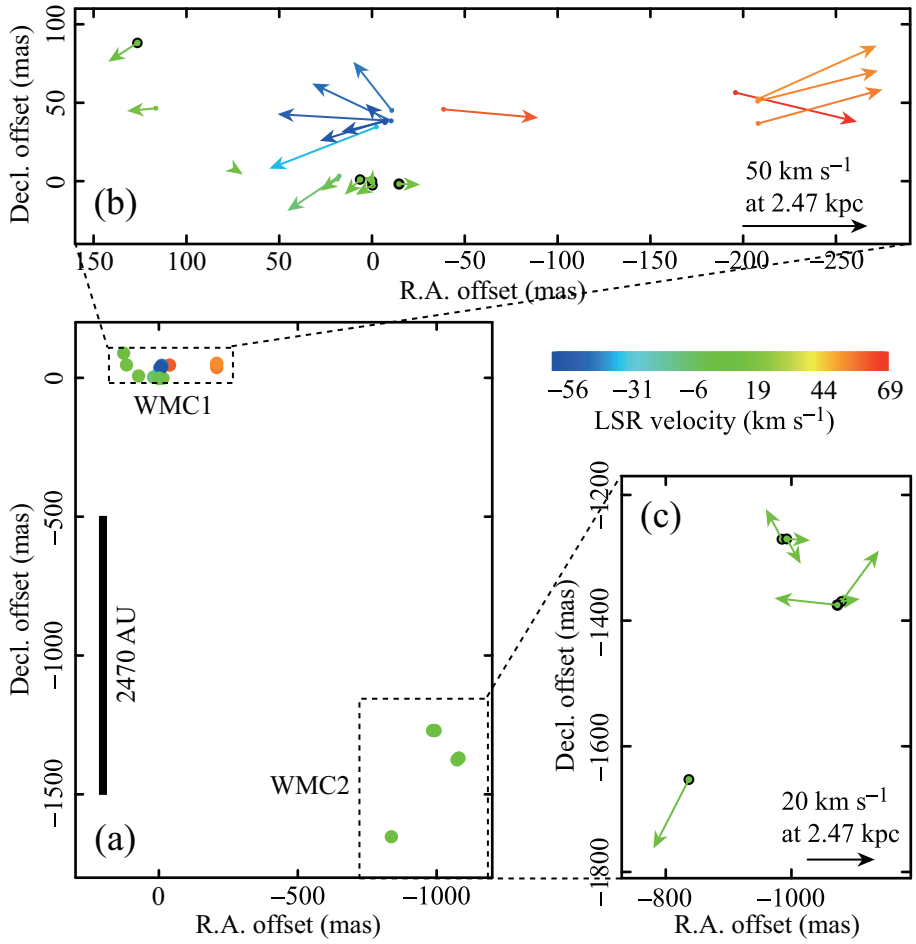

Fig. 2. (a): Distributions of H_2O masers in ON1. The color index denotes the LSR velocity range from -56.8 to 69.6 km s^{-1}, where 28 features are located. The map origin is located at the position of the reference maser feature at $v_{\rm LSR} = 14.9$ km s^{-1}, and $(\alpha,\delta)_{\rm J2000} = (20^{\rm h}10^{\rm m}09\overset{\rm s}{.}20454, 31^\circ31'36\overset{''}{.}1012)$ in 2006/245. (b), (c): Close-up to the two maser clusters (WMC1 and WMC2) with internal proper-motion vectors. The maser features measured the parallax and proper motions are highlighted by black circle.

Bronfman et al. 1996). The absolute proper motions of ten maser features are range from -3.89 to -2.05 mas yr^{-1} in right ascension and from -5.58 to -3.15 mas yr^{-1} in declination. From the average (the arithmetic mean) of these values the systemic proper motion of ON1 is derived to be $(\mu_\alpha\cos\delta, \mu_\delta) = (-3.10\pm0.18, -4.70\pm0.24)$ mas yr^{-1}, where the error is the standard error of the mean. Although there is a difference of approximately 1 mas yr^{-1} between the averaged proper motions of WMC1 and WMC2, it would be the relative stellar motion since WMC1 and WMC2 are associated with the different sources. Averaging the motions of multiple sources can also help to determine the systemic motion of ON1. We compared to the proper motion obtained by Rygl et al. (2010). Rygl et al. (2010) measured the proper motions of ON1 using the two background sources, J2003+3034 and J2009+3049, and obtained the different proper motions between them because of their apparent movements. Our derived systemic proper motion is close to the proper motion obtained using J2009+3049.

We convert the proper motion of $(\mu_\alpha\cos\delta, \mu_\delta) = (-3.10\pm0.18, -4.70\pm0.24)$ mas yr^{-1} to one with respect to LSR using the Solar motion in the traditional definition of $(U_\odot, V_\odot, W_\odot) = (10.3, 15.3, 7.7)$ km s^{-1}. In the previous studies for the astrometry of the Galactic maser sources, the Solar motion of $(U_\odot, V_\odot, W_\odot) = (10.00, 5.25, 7.17)$ km s^{-1} based on the HIPPARCOS satellite data (Dehnen & Binney 1998) is widely used. However, Schönrich, Binney, & Dehnen (2010) suggest that the value of $V_\odot$ determined by Dehnen & Binney (1998) is underestimated by ~ 7 km s^{-1}, and show the value which is close to the value of the traditional definition used in this study. Using the Galactic coordinate of ON1 $(l, b) = (69\overset{\circ}{.}54, -0\overset{\circ}{.}98)$, the proper motion with respect to LSR projected to the direction of l and b is calculated to be $(\mu_l, \mu_b) = (-6.00\pm0.22, 0.69\pm0.20)$ mas yr^{-1}. This proper motion corresponds to a velocity of $(v_l, v_b) = (-70.2\pm2.6, 8.1\pm2.3)$ km s^{-1}.

4. Discussion

As shown in section 1, the source at the tangent point has a kinematically unique property and one of the key objects to study the kinematics and geometry of the MWG.

Table 1. The best-fit values of parallax and proper motions for ten H_2O maser features in ON1.

ID	$\Delta\alpha$ (mas)	$\Delta\delta$ (mas)	$v_{\rm LSR}$ (km s^{-1})	Detected epochs	π (mas)	$\mu_\alpha \cos\delta$ (mas yr^{-1})	μ_δ (mas yr^{-1})
1	126.5	88.1	7.7	11111111100	0.389 ± 0.036	-2.65 ± 0.09	-5.58 ± 0.12
2	6.5	1.1	10.2	00011111111	0.428 ± 0.025	-2.73 ± 0.05	-5.44 ± 0.08
3	0.0	0.0	14.9	11111111111	0.407 ± 0.021	-3.42 ± 0.03	-5.30 ± 0.04
4	-0.2	-2.6	14.4	01111111110	0.420 ± 0.041	-3.32 ± 0.05	-5.21 ± 0.07
5	-14.6	-1.8	16.5	11111111111	0.382 ± 0.031	-3.89 ± 0.07	-4.94 ± 0.09
6	-836.8	-1653.0	10.6	11111111111	0.421 ± 0.066	-3.20 ± 0.09	-5.02 ± 0.12
7	-985.1	-1270.3	14.0	11111111000	0.390 ± 0.055	-3.51 ± 0.10	-4.08 ± 0.14
8	-994.3	-1269.9	6.4	11111100000	0.382 ± 0.057	-3.71 ± 0.15	-3.15 ± 0.21
9	-1073.2	-1375.1	8.5	11111110000	0.399 ± 0.039	-2.05 ± 0.11	-3.72 ± 0.16
10	-1079.9	-1369.5	7.3	00111111110	0.416 ± 0.065	-2.51 ± 0.15	-4.58 ± 0.20
		Combined fit			0.404 ± 0.012		
		Average				-3.10 ± 0.18	-4.70 ± 0.24

Column (2), (3): Offsets relative to the positon of the maser feature at $v_{\rm LSR} = 14.9$ km s^{-1}, and $(\alpha, \delta)_{\rm J2000} = (20^{\rm h}10^{\rm m}09\overset{\rm s}{.}20454, 31°31'36\overset{''}{.}1012)$ in 2006/245.
Column (4): LSR velocity.
Column (5): Detected epochs: '1' for detection, and '0' for non-detection.
Column (6): Parallax estimates.
Column (7), (8): Motions on the sky along the right ascension and declination.

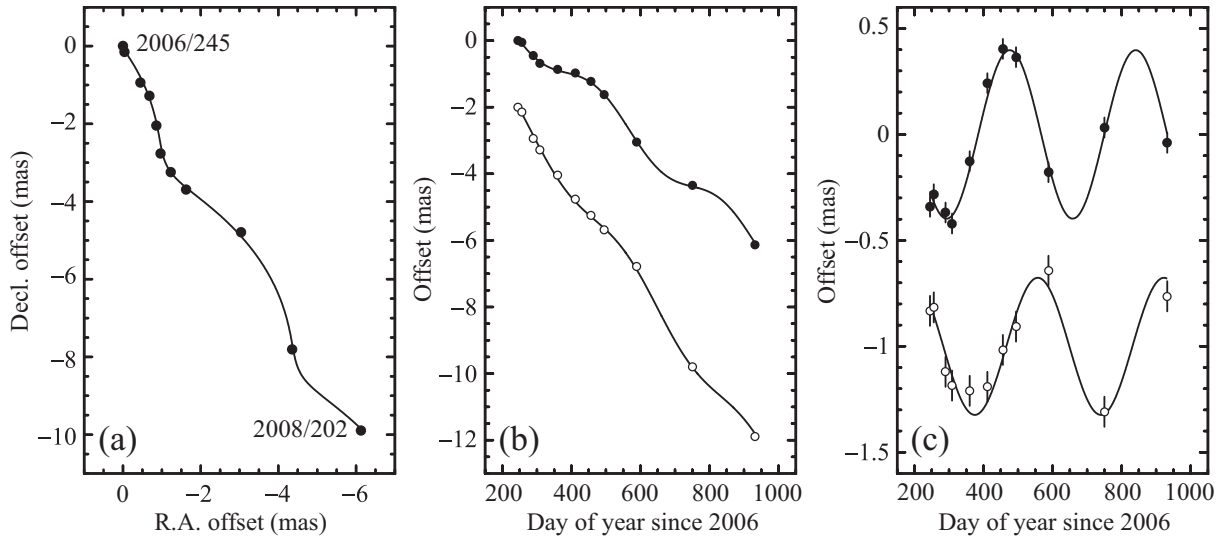

Fig. 3. Parallax and proper motion data and fits for the maser feature of $v_{\rm LSR} = 14.9$ km s^{-1}. (a): Positions on the sky with first and last epochs labeled. Solid line indicates the parallax and proper motion fit. (b): x (filled circles) and y (open circles) position offsets versus time. Solid line indicates the parallax and proper motion fit. The y data have been offset from the x data for clarity. (c): same as (b) panel, expect the proper motion fit has been removed, allowing the effects of only the parallax to be seen.

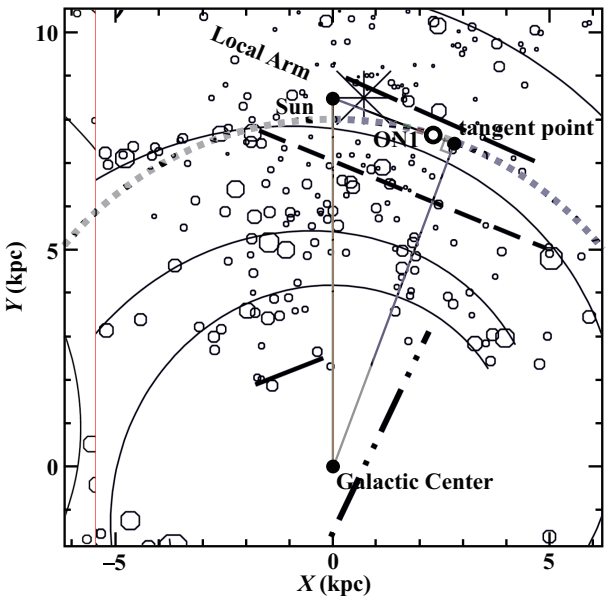

Fig. 4. Position of the ON1 in the MWG. The background is the four spiral arm structure of the MWG (Russeil 2003). The thick lines sketched by Russeil (2003) show the local arm feature (long dashed line), the bar orientation and length (dashed-dot-dot line) from Englmaier & Gerhard (1999), the expected departure from a logarithmic spiral arm observed for the Sagittarius-Carina arm (short dashed line), and a feature certainly linked to the three-kpc arm (solid line).

Due to a symmetric geometry, the radial velocity of a source at the tangent point with a pure circular rotation is equal to the terminal velocity.

The radial velocity of ON1 observed in molecular lines is 12 ± 1 km s^{-1} (Bronfman et al. 1996; Pankonin et al. 2001), The terminal velocity at $l = 69.^{\circ}54$ is 15 ± 5 km s^{-1} (Dame et al. 2001). They are the same within the error. This suggests that ON1 is located at the tangent point. In the case that the source is located exactly at the tangent point, and it is on pure circular rotation, the source, Sun, and the Galactic center make the right triangle, and the source proper motion on the sky depends only on the Galactic rotation of Sun. This geometry is shown in Figure 5(a). Therefore, R_0 and Θ_0 are determined from the observed distance to the source, D, and the proper motion on the sky along the Galactic plane, v_l, as

$$R_0 = D/\cos l \tag{1}$$

$$\Theta_0 = -v_l/\cos l. \tag{2}$$

The Galactic constants are estimated to be $R_0 = 7.1 \pm 0.3$ kpc and $\Theta_0 = 201 \pm 7$ km s^{-1}, respectively, from $D = 2.47 \pm 0.11$ kpc and $v_l = -70.2 \pm 2.6$ km s^{-1}. These values are approximately 10–20% smaller than the IAU recommended values of $R_0 = 8.5$ kpc and $\Theta_0 = 220$ km s^{-1}, the recently estimated values of $R_0 = 8.4 \pm 0.6$ kpc and $\Theta_0 = 254 \pm 16$ km s^{-1} (Reid et al. 2009), and $R_0 = 8.3 \pm 1.1$ kpc estimated using the parallax measurement of W51 Main/South located near the tangent point (Sato et al. 2010).

However, our estimated R_0 and Θ_0 would not be inconsistent with the previous estimates. This is because our estimation is affected by the ambiguities of the two assumptions that ON1 is on the pure circular rotation, and located exactly at the tangent point. We evaluate these effects. Since the velocity deviation of the molecular cloud in ON1 is estimated to be 3–8 km s^{-1} from the full width at half maximum of the profiles in molecular lines (Zheng et al. 1985; Haschick & Ho 1990; Bronfman et al. 1996), the maser source in ON1 may have the peculiar motion of the similar velocity. If we allow for this peculiar motion of 3–8 km s^{-1}, the errors of our estimated R_0 and Θ_0 are larger than 10–20%. In the case that we use the IAU recommended values of $R_0 = 8.5$ kpc and $\Theta_0 = 220$ km s^{-1}, and assume the flat rotation, the peculiar motion is estimated to be $(U', V', W') = (7.0 \pm 2.5, -1.8 \pm 1.3, 8.1 \pm 2.3)$ km s^{-1} from the measured distance, proper motion, and radial velocity using the method shown in Reid et al. (2009). Here, U' is the velocity component toward the Galactic Center, V' is the component in the direction of the Galactic rotation, W' is the component toward the north Galactic pole. In the case that we use different Galactic constants of $R_0 = 8.4$ kpc and $\Theta_0 = 254$ km s^{-1} (Reid et al. 2009), the peculiar motion is estimated to be $(U', V', W') = (-3.7 \pm 2.5, -3.2 \pm 1.3, 8.1 \pm 2.3)$ km s^{-1}. In both cases, the peculiar motion velocity is in the range of the velocity deviation of the molecular cloud. There may be a velocity difference of approximately 5 km s^{-1} between the radial velocity and the terminal velocity, considering their errors. If this velocity difference is due to the offset from the tangent point to ON1, this offset is estimated to be approximately ± 1.7 kpc. If ON1 is not located exactly at the tangent point and there is a offset of ± 1.7 kpc between them, the errors of our estimated R_0 and Θ_0 increase to approximately 70%.

Although the estimated values of the Galactic constants are strongly affected by the assumption of the source location in the MWG. However we found that the ratio of Galactic constants, Θ_0/R_0, the angular velocity of Galactic rotation at Sun, Ω_0, can be estimated with small ambiguity. In the case that the source is on pure circular rotation at any position in the Galactic disk, the radial and tangential velocities of the source can be written as

$$v_r = \left(\frac{\Theta}{R} - \frac{\Theta_0}{R_0}\right) R_0 \sin l, \tag{3}$$

$$v_l = \left(\frac{\Theta}{R} - \frac{\Theta_0}{R_0}\right) R_0 \cos l - \frac{\Theta}{R} D. \tag{4}$$

From these equations, the relation between the Θ_0 and R_0 is obtained to be

$$\begin{aligned}\Theta_0 &= \left[-\frac{v_l}{D} + v_r\left(\frac{1}{D\tan l} - \frac{1}{R_0 \sin l}\right)\right] R_0 \\ &= \left[-a_0\mu_l + v_r\left(\frac{1}{D\tan l} - \frac{1}{R_0 \sin l}\right)\right] R_0,\end{aligned} \tag{5}$$

where a_0 is a conversion constant from a proper motion to a linear velocity (4.74 km s^{-1} mas^{-1} yr kpc^{-1}). The equation (5) is graphed in Figure 6(a) using the observed

values of $D = 2.47 \pm 0.11$ kpc, $\mu_l = -6.00 \pm 0.22$ mas yr^{-1}, and $v_r = 12 \pm 1$ km s^{-1}. We found that the slope in Figure 6(a) is a nearby constant at $7 \leq R_0 \leq 9$ kpc. The slope yields the ratio Θ_0/R_0, which is described as

$$\frac{\Theta_0}{R_0} = -\frac{v_l}{D} + v_r \left(\frac{1}{D \tan l} - \frac{1}{R_0 \sin l} \right) = -a_0 \mu_l + v_r \left(\frac{1}{D \tan l} - \frac{1}{R_0 \sin l} \right), \quad (6)$$

The equation (6) is graphed in Figure 6(b). The ratio is estimated to be $\Theta_0/R_0 = 28.7 \pm 1.3$ km s^{-1} kpc^{-1} using the above observed values, and $7 \leq R_0 \leq 9$ kpc. The error of Θ_0/R_0 mainly depends on that of μ_l. The errors of Θ_0/R_0 depend on those of v_r and D are ± 0.02 and ± 0.05 km s^{-1} kpc^{-1}, respectively, and they can be neglected in this estimation. This is because that $D \tan l \simeq R_0 \sin l$ in the case that the source is located near the tangent point (see Figure 5(b)). We adopted $7 \leq R_0 \leq 9$ kpc in this estimation. This means that ON1 is located within -0.02–0.68 kpc from the tangent point, because the offset from the tangent point is written as $\Delta D = R_0 \cos l - D$.

Our estimated ratio $\Theta_0/R_0 = 28.7 \pm 1.3$ km s^{-1} kpc^{-1} is close to the value of 27.3 ± 0.8 km s^{-1} kpc^{-1} obtained from the parallax and proper motion measurement of ON2N which is located on the Solar circle (Ando et al. 2010, submitted to PASJ). Our estimated ratio is consistent with the value of $\Theta_0/R_0 = 29.45 \pm 0.15$ km s^{-1} estimated from the proper motion measurement of Sgr A* (Reid & Brunthaler 2004). Reid & Brunthaler (2004) adopt the Solar motion in the direction of Galactic rotation of $V_\odot = 5.25$ km s^{-1} (Dehnen & Binney 1998). We adopt the Solar motion in the traditional definition of $(U_\odot, V_\odot, W_\odot) = (10.3, 15.3, 7.7)$ km s^{-1} (see subsection 3.2). The error of our estimated ratio depends on that of $V_\odot$ is estimated to be ± 1.4 km s^{-1} kpc^{-1} from $V_\odot = 15 \pm 10$ km s^{-1}. Even if we consider this, our estimated value is larger than the IAU recommended value of 220 km s^{-1}/8.5 kpc = 25.9 km s^{-1} kpc^{-1}.

We can find the other sources which is expected to be located at the tangent point from the Arcetri catalog of H_2O maser (Valdettaro et al. 2001). Therefore, we will observe these sources with VERA, in order to determine the Galactic constants and the angular rotation velocity of the Galactic rotation at Sun.

We are grateful to an anonymous referee for valuable comments and suggestions. We thank to the staff members of all the VERA stations for their assistances in the observations.

References

Ando, K., et al. 2010, submitted to PASJ
Bronfman, L., Nyman, L.-A., & May, J. 1996, A&AS, 115, 81
Dame, T. M., Hartmann, D., & Thaddeus, P. 2001, ApJ, 547, 792
Dehnen, W., & Binney, J. J. 1998, MNRAS, 298, 387
Englmaier, P., & Gerhard, O. 1999, MNRAS, 304, 512
Fomalont, E. B., Petrov, L., MacMillan, D. S., Gordon, D., & Ma, C. 2003, AJ, 126, 2562
Hachisuka, K., et al. 2006, ApJ, 645, 337
Haschick, A. D., & Ho, P. T. P. 1990, ApJ, 352, 630
Honma, M., et al. 2007, PASJ, 59, 889
Honma, M., et al. 2008, PASJ, 60, 935
Honma, M., Tamura, Y., & Reid, M. J. 2008, PASJ, 60, 951
Iguchi, S., Kurayama, T., Kawaguchi, N., & Kawakami, K. 2005, PASJ, 57, 259
McMillan, P. J., & Binney, J. J. 2010, MNRAS, 402, 934
Nagayama, T., Nakagawa, A., Imai, H., Omodaka, T., & Sofue, Y. 2008, PASJ, 60, 183
Pankonin, V., Churchwell, E., Watson, C., & Bieging, J. H. 2001, ApJ, 558, 194
Reid, M. J., & Brunthaler, A. 2004, ApJ, 616, 872
Reid, M. J., et al. 2009, ApJ, 700, 137
Russeil, D. 2003, A&A, 397, 133
Rygl, K. L. J., Brunthaler, A., Reid, M. J., Menten, K. M., van Langevelde, H. J., & Xu, Y. 2010, A&A, 511, A2
Sato, M., Reid, M. J., Brunthaler, A., & Menten, K. M. 2010, ApJ, 720, 1055
Schönrich, R., Binney, J., & Dehnen, W. 2010, MNRAS, 403, 1829
Valdettaro, R., et al. 2001, A&A, 368, 845
Xu, Y., Reid, M. J., Zheng, X. W., & Menten, K. M. 2006, Science, 311, 54
Zheng, X. W., Ho, P. T. P., Reid, M. J., & Schneps, M. H. 1985, ApJ, 293, 522

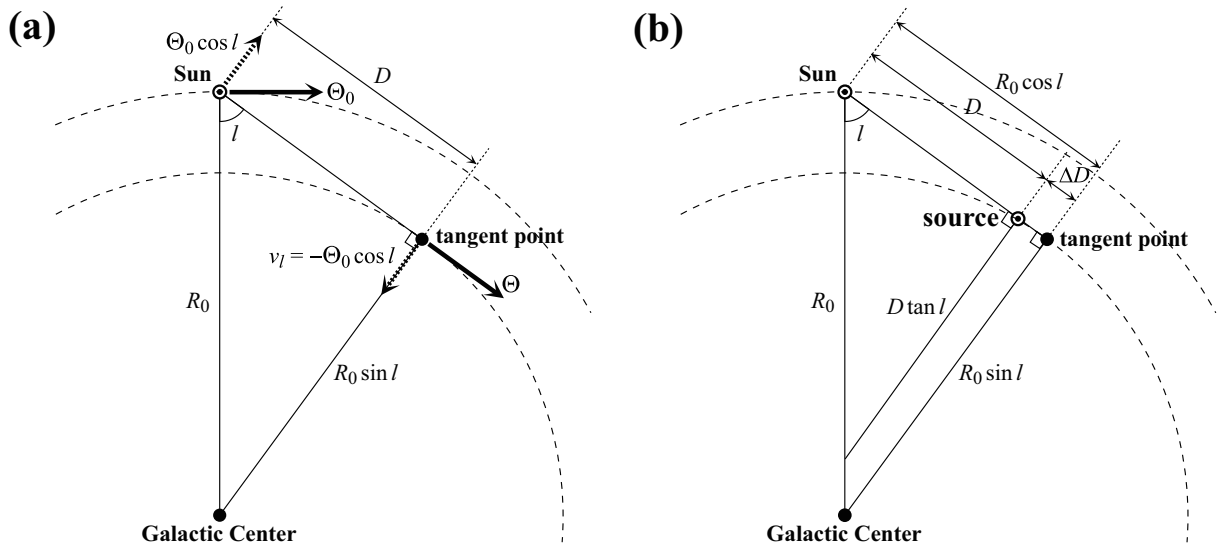

Fig. 5. The geometry of the Galactic center, Sun, the tangent point, and the source. (a): The geometry in the case that the source is located at the tangent point. (b): The geometry in the case that there is a offset between the source and the tangent point.

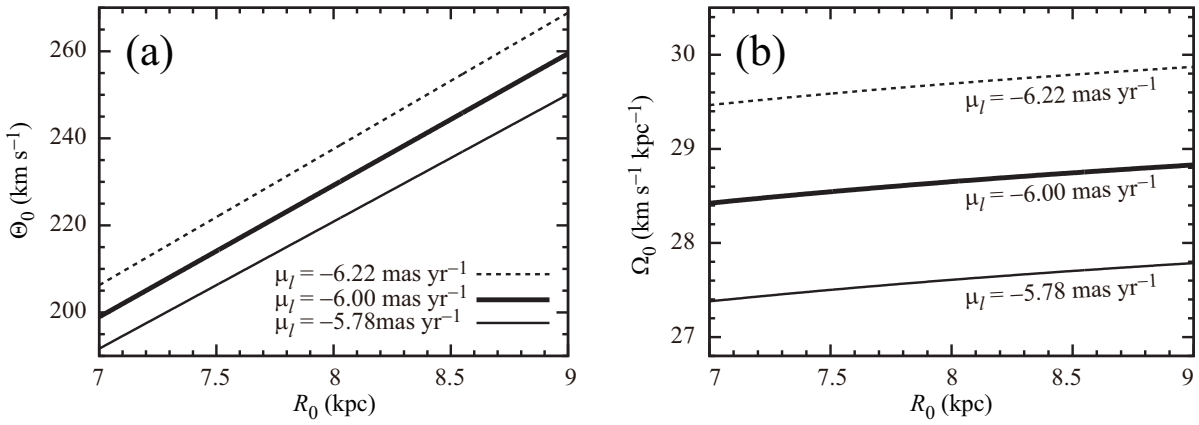

Fig. 6. (a): The relation of R_0 and Θ_0 shown in the equation (5). (b): The relation of R_0 and Θ_0/R_0 shown in the equation (6).